THE JOURNAL OF BIOLOGICAL CHEMISTRY VOL. 284, NO. 21, pp. 14503–14512, May 22, 2009

Glutamate Binding and Conformational Flexibility of Ligand-binding Domains Are Critical Early Determinants of Efficient Kainate Receptor Biogenesis

Received for publication, January 22, 2009, and in revised form, March 13, 2009 Published, JBC Papers in Press, April 2, 2009, DOI 10.1074/jbc.M900510200

Martin B. Gill[‡], **Pornpun Vivithanaporn**[§¶], **and Geoffrey T. Swanson**[‡1]

From the [‡]*Department of Molecular Pharmacology and Biological Chemistry, Northwestern University, Feinberg School of Medicine, Chicago, Illinois 60611, the* [§]*Department of Pharmacology, Faculty of Science, Mahidol University, Bangkok 10400, Thailand, and the* [¶]*Department of Neurology, University of Alberta, Edmonton, Alberta T6G 2S2, Canada*

Intracellular glutamate binding within the endoplasmic reticulum (ER) is thought to be necessary for plasma membrane expression of ionotropic glutamate receptors. Here we determined the importance of glutamate binding to folding and assembly of soluble ligand-binding domains (LBDs), as well as full-length receptors, by comparing the secretion of a soluble GluR6-S1S2 protein *versus* the plasma membrane localization of GluR6 kainate receptors following mutagenesis of the LBD. The mutations were designed to either eliminate glutamate binding, thereby trapping the bilobate LBD in an "open" conformation, or "lock" the LBD in a closed conformation with an engineered interdomain disulfide bridge. Analysis of plasma membrane localization, medium secretion of soluble LBD proteins, and measures of folding efficiency suggested that loss of glutamate binding affinity significantly impacted subunit protein folding and assembly. In contrast, receptors with conformationally restricted LBDs also exhibited decreased PM expression and altered oligomeric receptor assembly but did not exhibit any deficits in subunit folding. Secretion of the closed LBD protein was enhanced compared with wild-type GluR6-S1S2. Our results suggest that glutamate acts as a chaperone molecule for appropriate folding of nascent receptors and that relaxation of LBDs from fully closed states during oligomerization represents a critical transition that necessarily engages other determinants within receptor dimers. Glutamate receptor LBDs therefore must access multiple conformations for efficient biogenesis.

Cellular control over the biogenesis and trafficking of ionotropic glutamate receptors (iGluRs)[2] probably constitutes a major regulatory process that prevents aberrant excitatory neurotransmission within the central nervous system. Many receptor trafficking determinants are genetically encoded within the primary amino acid sequences of cytoplasmic carboxyl-terminal domains of iGluR subunits (1, 2). Association of these determinants with accessory or chaperone proteins enhances forward transit from the endoplasmic reticulum (ER), insertion into the plasma membrane (PM), synaptic targeting, or a variety of other trafficking processes (3–6). Ligand binding and gating domains upstream of carboxyl-terminal domains also are critical in biogenesis of iGluRs (7–11). Elucidating how these domains are engaged as quality control checkpoints is essential to developing a comprehensive understanding of the neuronal mechanisms for control of excitatory transmission in the central nervous system.

Several recent studies have proposed that intracellular glutamate binding within the ER promotes proper folding and maturation of AMPA and kainate receptors and is required for forward trafficking of fully assembled receptors (10, 12–15). This hypothesis is based in large part on the observation that mutagenesis of key glutamate-binding residues in the LBD greatly reduces or eliminates PM localization (7, 10, 12, 13); the mechanistic basis of this putative quality control process is not understood. The critical receptor determinants involved in these cellular checkpoints could reside in the LBD, in other regions that undergo glutamate-dependent alterations in structure, or in intersubunit interactions associated with receptor desensitization (7–10, 16). It is possible that glutamate binding to iGluRs (and subsequent conformational rearrangements) act as tests of the functionality of fully assembled, export-ready receptors (8, 12, 16); alternatively, intact glutamate-binding sites may be required for earlier steps in receptor biogenesis, such as subunit folding and oligomeric assembly (7, 16).

We tested here whether the glutamate-dependent conformational changes critical to GluR6a KAR cell surface expression are restricted solely to the bilobate LBD, formed by the S1 and S2 segments of the receptor protein, or instead involve additional domains in the KAR subunits. Toward that end, we compared the effect of an LBD mutation that eliminated binding affinity for glutamate, T690A, on the efficiency of secretion of a soluble GluR6-S1S2 protein *versus* PM localization of the full-length receptor; this served as one way to test the autonomy of the LBD in quality control processes, because soluble LBDs fold properly, form binding sites similar to those in the full-length receptor, and transit the secretory pathway to be released into culture media. Furthermore, we trapped LBDs of full-length receptors and soluble GluR6-S1S2 proteins in conformations that mimic closed, glutamate-bound states by introduction of a reversible, interdomain (D1-D2) disulfide bond,

[1] To whom correspondence should be addressed: Dept. of Molecular Pharmacology and Biological Chemistry, Northwestern University, Feinberg School of Medicine, Searle 7-443, 303 E. Chicago Ave., Chicago, IL 60611. Tel.: 312-503-1052; Fax: 312-503-1402; E-mail: gtswanson@northwestern.edu.

[2] The abbreviations used are: iGluR, ionotropic glutamate receptor; ER, endoplasmic reticulum; PM, plasma membrane; LBD, ligand-binding domain; ELISA, enzyme-linked immunosorbent assay; DPBS, Dulbecco's phosphate-buffered saline; DTT, dithiothreitol; BN-PAGE, blue native PAGE; GFP, green fluorescent protein.

allowing us to test the role of LBD relaxation or flexibility in assembly and trafficking. We found that the ligand binding mutation resulted in reduced maturation and receptor surface expression in part through misfolding of the LBD. In addition, we found that locking the LBD into a closed state reduced receptor maturation and expression but that this engaged regions outside of the LBD. Although the locked, closed mutant also had assembly defects that occurred at the transition from dimers to tetramers, these did not result from apparent folding defects, suggesting that relaxation or opening of the LBD represents a critical step during oligomerization. In summary, we propose that LBDs must be able to access multiple conformations for efficient KAR biogenesis.

EXPERIMENTAL PROCEDURES

Molecular Biology—All cDNAs were in pcDNA3 vectors. Unedited Myc-GluR6a(Q) cDNA was received from Dr. Christophe Mulle (Université Bordeaux II, France). cDNA for the soluble GluR6-S1S2 LBD protein was received from Mark Mayer (National Institutes of Health, Bethesda, MD), and the M3-S2 linker region, FLTVERMES (full-length receptor corresponding to amino acids 627–635), was inserted N-terminal to the S2 sequence. This insertion was made to allow for the study of the potential role for the M3-S2 linker in LBD function in a previous study and was maintained for consistency of data (7). Six c-Myc epitopes were added C-terminal to the histidine codon of the signal peptide. For clarity, residues in the soluble S1S2 protein are referred to by the analogous amino acid in the full-length receptor. Amino acid numbering in the full-length receptor starts with the initiation methionine (8, 10). All point mutations were made using the QuikChange site-directed mutagenesis protocol (Stratagene, La Jolla, CA) and were confirmed via DNA sequencing.

Cell Culture and Transfection—COS-7 cells (CRL-1651; American Type Culture Collection, Manassas, VA) and human embryonic kidney cells expressing T-antigen, clone 17 (HEK293-T/17) (CRL-11268) were cultured in DMEM supplemented with 100 μg/ml penicillin, 100 μg/ml streptomycin, and 10% heat-inactivated fetal bovine serum at 37 °C with 5% CO_2. Cells were fed every other day and split twice per week. 24 h prior to transfection, cells were plated at 3×10^4 cells/cm^2 in fresh medium. Cells were transfected with wild-type or mutant GluR6 cDNAs using Mirus Trans-IT transfection reagent (Mirus Bio Corp., Madison, WI) at a ratio of 1 μg of cDNA/3 μl Trans-IT reagent and maintained in transfection medium until the completion of the assay.

ELISA—Cells in duplicate 12-well plates were transfected with 0.6 μg/well of cDNA. 48 h post-transfection, cells were washed twice in ice-cold Dulbecco's phosphate-buffered saline (DPBS) and fixed with 4% paraformaldehyde for 20 min at room temperature. After fixation, cells were washed three times in DPBS. For surface staining, fixed cells were then incubated in mouse α-c-Myc antibody (1.6 μg/ml, clone 9E10; Roche Applied Sciences) in 10% normal goat serum for 1 h at room temperature. For total staining, fixed cells were first permeabilized for 10 min at room temperature with 0.2% Triton X-100/DPBS and then incubated with mouse α-c-Myc antibody for 1 h at room temperature. Both groups were washed three times with DPBS and then incubated with horseradish peroxidase-conjugated goat α-mouse secondary antibody (1:1000, NA931V; GE Healthcare) in 10% normal goat serum for 1 h at room temperature. Cells were again washed three times in DPBS and then incubated in the horseradish peroxidase substrate, SIGMA*FAST* OPD (P9187; Sigma) for 1 h in the dark at room temperature. The optical density of 200 μl of incubation medium was detected at 490 nm using a spectrophotometer. For experiments involving DTT treatment, at 32 h post-transfection, cells for both surface and total wells were incubated for 16 h with 1 mM DTT at 37 °C in 5% CO_2. All values were an average of triplicate samples from each well, and the background absorbances from untransfected well O.D. readings were subtracted from each sample. Data are presented as a percentage of surface/total absorbance ratios.

Glycosidase Resistance Assay—Medium from cells transfected 24 h with Myc-GluR6-S1S2 cDNA was replaced with fresh medium and incubated for an additional 24 h. From this medium, 50 μg of Myc-GluR6-S1S2-containing medium were digested with no glycosidase, endoglycosidase H (P0702S; New England Bio1abs, Ipswich, MA), or peptide:*N*-glycosidase F (P0704S; New England Biolabs) in the provided reaction buffers for 1 h at 37 °C according to the manufacturer's protocol. These digested samples were then run on a 10% SDS-polyacrylamide gel. Undigested and digested bands were detected with a mouse α-c-Myc antibody (0.4 μg/ml; Roche Applied Sciences) and horseradish peroxidase-conjugated goat α-mouse secondary antibody (1:2000; GE Healthcare). Densitometric analysis was carried out on the film using NIH ImageJ, and the data are represented as a ratio of the resistant band to the undigested band.

Electrophysiology—HEK293-T/17 cells were co-transfected with 0.2 μg of wild-type or mutant Myc-GluR6a cDNA and 0.05 μg of enhanced GFP. 48 h post-transfection, transfected cells were lifted from the coverslip and recorded in whole cell voltage clamp mode. Whole cell patch clamp recordings were performed as previously described (17). The extracellular solution contained 140 mM NaCl, 10 mM HEPES (pH 7.3), 10 mM glucose, 3 mM KCl, 2 mM $CaCl_2$ and 1 mM $MgCl_2$. The internal solution contained 110 mM CsCl, 30 mM CsF, 10 mM HEPES (pH 7.3), 4 mM NaCl, 0.5 mM $CaCl_2$, and 5 mM EGTA. Borosilicate path electrodes were pulled and fire-polished to 2–4 megaohms resistance. Lifted cells were maintained in a laminar stream of extracellular solution from a triple-barreled flow pipe for fast application of 10 mM glutamate (the 10–90% rise time of glutamate-evoked currents was ~1 ms).

Western Blot Analysis—COS-7 cells were washed twice with DPBS and lysed in lysis buffer (containing 150 mM NaCl, 50 mM Tris (pH 7.3), 0.5% Nonidet P-40, and protease inhibitor mixture (P2714; Sigma)) for 10 min on ice. Crude homogenates were centrifuged for 20 min at 20,000 $\times$ *g*, and the supernatant was collected as total cellular protein. 10 μg of protein were boiled for 10 min in 2$\times$ Laemmli buffer (catalog number 161-0737; Bio-Rad) and 350 mM β-mercaptoethanol (catalog number 161-0710; Bio-Rad), separated on a 7.5% SDS-polyacrylamide gel, and transferred overnight to a nitrocellulose membrane. Membranes were blocked in 5% nonfat dried milk in TBS-T (Tris-buffered saline, pH 7.3, and 0.05% Tween 20 (P9416;

Sigma)) for 2 h, washed twice in TBS-T, and then incubated for 1–2 h at room temperature in mouse α-c-Myc primary antibody (0.4 μg/ml; Roche Applied Sciences) diluted in blocking buffer. After washing, membranes were incubated in horseradish peroxidase-conjugated goat α-mouse secondary antibody at room temperature for 1 h (1:5000; GE Healthcare) diluted in blocking buffer. Membranes were washed and incubated for 5 min at room temperature in SuperSignal West Pico chemiluminescent substrate (Thermo Scientific, Rockford, IL). Densitometric analysis was performed using ImageJ software (National Institutes of Health).

Blue Native Polyacrylamide Gel Electrophoresis (BN-PAGE)—For analysis of receptor assembly, protein from transfected wells at 18 and 24 h post-transfection was collected as described above. Then samples were subjected to BN-PAGE, as described (18). Briefly, 10 μg of protein were loaded without boiling in 2× BN-PAGE loading buffer (final loaded solution containing 0.125% Coomassie Brilliant Blue G (B5133; Sigma), 10% glycerol, 0.01% bromphenol blue, and 62.5 mM Tris (pH 6.8)) and separated on precast non-SDS 4–15% Tris gels (161–1104; Bio-Rad) for 45 min at 100 V, 45 min at 150 V, and 200 V for 1 h at 4 °C. The anode buffer contained 250 mM Tris base, 1.92 M glycine, and the cathode buffer was identical to the anode buffer plus 0.004% Coomassie Brilliant Blue G. Proteins were transferred overnight to a polyvinylidene difluoride membrane, and the membranes were blocked in 5% nonfat dried milk in TBS-T overnight at 4 °C. Membranes were washed twice in TBS-T and then incubated overnight in mouse α-c-Myc primary antibody (0.2 μg/ml; Roche Applied Sciences) at 4 °C. Following another three washes, membranes were incubated in horseradish peroxidase-conjugated goat α-mouse secondary antibody (1:4000) for 1 h at room temperature and analyzed using the same techniques as described for Western blots. Data are presented as a ratio of the optical densities for the oligomeric states of the mutant and wild-type Myc-GluR6a(Q) receptors.

Fluorescence Recovery after Photobleaching—To measure the ER mobility of the GFP-GluR6a(Q), cells were plated in glass bottom (number 1.5) 35-mm dishes (P35G-1.5-14-C; Matek, Ashland, MA) and transfected with the respective GFP-tagged receptors. To disrupt the Golgi network, cells were incubated with brefeldin A for 4 h (2 μg/ml; Sigma) at 37 °C in 5% CO_2 until imaging. At 48 h post-transfection, the medium was switched to Hanks' balanced salt solution with 15 mM HEPES (pH 7.3), and cells were depleted of ATP by incubation for 60 min in 50 μM 2-deoxyglucose and 0.02% sodium azide at 37 °C in 5% CO_2, as described previously (19). Live cells expressing the GFP-tagged receptor were then subjected to photobleaching. Immediately prior to photobleaching, an image was captured of the live cell at 17.9% transmission of a 20-milliwatt helium-neon laser at 70% power with a pinhole size of 3 Airy units on a Zeiss LSM 510 Meta confocal microscope (Carl Zeiss) within the Northwestern University Cell Imaging Facility. A small circular region of the same diameter was used for each cell, and the area was photobleached by 50 iterations at 100% transmission. Immediately after photobleaching, another image was collected at 17.9% transmission and every 12 s thereafter until fluorescence within the photobleached area had reached a steady state level. Analysis was performed using ImageJ software. Background was subtracted from each image in the series, and fluorescence for both the photobleached region and the whole cell was collected at each time point. Cells were not included if the whole cell fluorescence did not reach an asymptote (*i.e.* continuous photobleaching occurred). The following formulas, based on methodology described by Lippincott-Schwartz (20), were used to calculate mobile fraction (M_f), fractional fluorescence (F_f), and the effective diffusion coefficient (D_{eff}). For M_f, we used Equation 1,

$$M_f = 100 \times (F_{precell}/F_{final\ cell}) \times ((F_{final\ cell} - F_{postbleach\ area})/(F_{prebleach\ area} - F_{postbleach\ area}), \quad \text{(Eq. 1)}$$

where $F_{precell}$ represents the whole cell prebleach fluorescence, $F_{final\ cell}$ is the whole cell asymptote fluorescence, $F_{postbleach\ area}$ is the fluorescence within the photobleached area immediately after photobleaching, and $F_{prebleach\ area}$ is the fluorescence within the photobleached area immediately prior to photobleaching. Data are expressed as a percentage of the GFP-tagged receptor that is mobile. For fractional fluorescence, we used Equation 2,

$$F_f = 100 \times (F(t) - F_{postbleach\ area})/(F_{final\ area} - F_{postbleach\ area}), \quad \text{(Eq. 2)}$$

where $F(t)$ represents the fluorescence within the photobleached area at time t, $F_{postbleach\ area}$ is as described above, and $F_{final\ area}$ is the photobleached area asymptote fluorescence. Data were expressed as a percentage of final photobleached area fluorescence and were fit with a single exponential curve. Half-recovery time ($t_{1/2}$) was calculated as the time at which fluorescence reached half of the final fluorescence. For D_{eff}, we used Equation 3,

$$D_{eff} = 0.88 \times (r^2/4t_{1/2}), \quad \text{(Eq. 3)}$$

where r represents the radius of the photobleached area in μm, and $t_{1/2}$ is the half-recovery time in seconds (21). The D_{eff} is an estimation and assumes that 1) the area photobleached is circular and 2) movement only occurs in two dimensions.

Co-immunoprecipitation—48 h post-transfection, COS-7 cells plated in 100-mm dishes were lysed as described above, and 500 μg of protein was precleared by incubation overnight with 50 μl of protein A/G-Sepharose bead slurry (20421; Thermo Scientific) at 4 °C with end-over-end mixing. The beads were spun down, and the supernatant was incubated for 6–8 h at 4 °C with 4 μg of rabbit α-calnexin (SPA-860; Assay Designs, Ann Arbor, MI) with mixing. 50 μl of protein A/G-Sepharose bead slurry was added, and the solution was incubated with mixing overnight at 4 °C. The beads were spun down and washed three times with lysis buffer. The beads were then boiled for 6 min in 50 μl of 2× Laemmli buffer, and 15 μl of the eluate was separated on a 10% SDS-polyacrylamide gel. 2 μg of lysate protein was loaded for each respective construct. Proteins were transferred, blocked, and immunoblotted as described above. Optical densities for both the immunoprecipitated and lysate bands were measured, and data were represented as a percentage of the wild-type immunoprecipitated/lysate ratio.

Statistical Analysis—For data involving three or more groups, a one-way analysis of variance was performed with a Tukey-Kramer *post hoc* test for comparison among the groups. For data involving two groups, an unpaired Student's *t* test was performed; if the S.D. values between the two groups were statistically significant, a Welsh correction was added. For analysis of oligomerization, a two-way analysis of variance was performed with a Bonferroni *post hoc* test. Data are presented as mean ± S.E. with statistical significance set at $p < 0.05$.

RESULTS

Elimination of Glutamate Binding Reduces GluR6a Receptor Surface Expression—Mutation of the agonist binding site results in reduced plasma membrane expression of AMPA and kainate receptors (10, 12, 13, 15, 16). Here we tested whether the subunit determinants responsible for this reduced surface expression reside solely within the LBD or involve other domains within kainate receptor subunits. To that end, we compared the PM expression of the full-length GluR6a receptor to the secretion of a soluble protein (GluR6-S1S2), for wild-type and ligand binding-deficient GluR6 receptors. Mutation of threonine 690 eliminates a key hydrogen bond between the side chain hydroxyl group and the δ-carbonyl oxygen in glutamate and other receptor ligands, thereby reducing PM expression (10, 12). Similarly, we observed a significant reduction in the PM expression of GluR6a(T690A) (19.3 ± 6.0% of receptor protein was localized to the PM, $n = 7$) when compared with the wild-type GluR6a (76.6 ± 8.9%, $n = 7$, $p < 0.001$) (Fig. 1*A*, *bottom*). An analogous binding mutation in the soluble LBD protein, GluR6-S1S2(T690A), also reduced the relative secretion of the protein into the medium, albeit to a lesser degree than the reduction observed with the full-length receptor (to 65.7 ± 8.1% of the wild-type GluR6-S1S2, $n = 5$, $p < 0.05$) (Fig. 1*B*, *bottom*). A similar reduction in secretion occurs with a ligand binding-deficient GluR4 LBD (15). Thus, elimination of glutamate binding produced correlated reductions in GluR6a receptor surface expression and soluble LBD secretion, suggestive of a commonality in the cellular quality control processes disrupted by the binding site mutations.

An Interdomain Disulfide Bond in the LBD Reduces PM Expression of GluR6a Receptors—In order to test the importance of flexibility of the binding domain in receptor biogenesis, the LBD was "locked" in a closed conformation through cysteine mutagenesis of two amino acids, Glu^{441} and Asn^{721}, which form a critical interdomain hydrogen bond in the closed, agonist-bound LBD. The proximity of the side chains and their interaction in resolved, agonist-bound LBD structures suggested that an interdomain disulfide bridge would form and restrict rotation (22). A similar strategy was employed recently for GluR2 AMPA receptors (9). Plasma membrane expression of GluR6a(E441C/N721C) receptors was significantly lower than that of wild-type GluR6a receptors (27.8 ± 3.7%, $n = 14$ *versus* 75.4 ± 3.9%, $n = 13$, $p < 0.001$) (Fig. 2*A*, *bottom*). Analogous mutations were made in the soluble S1S2 protein, but in contrast to the full-length receptor, GluR6-S1S2(E441C/N721C) protein was secreted to a greater degree into the medium than wild-type GluR6-S1S2 protein (by 151.6 ± 11.9%, $n = 3$) (Fig. 2*B*, *bottom*). Thus, conformational restriction of the LBD with an intradomain disulfide bridge prevents receptor plasma membrane expression but promotes secretion of soluble LBD protein.

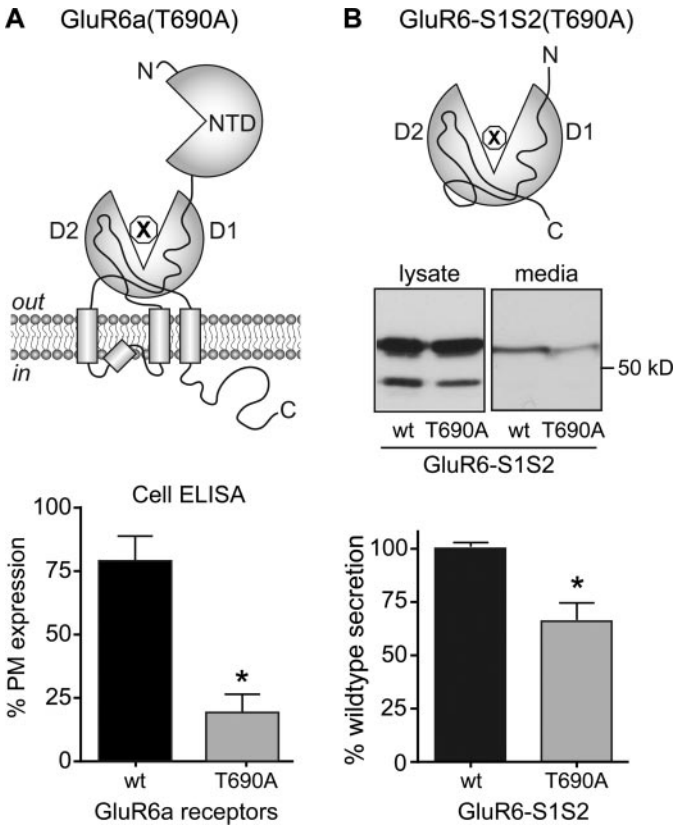

FIGURE 1. **Elimination of glutamate binding reduces GluR6a receptor surface expression.** *A*, *top*, diagram illustrating the domains of the full-length GluR6a receptor and the T690A ligand binding mutation. *Bottom*, quantification of cell ELISA data illustrating a reduction in PM expression resulting from the T690A LBD mutation (19.3 ± 6.0%, $n = 7$ *versus* 76.6 ± 8.9%, $n = 7$, $p < 0.001$). *B*, *top*, diagram illustrating the soluble GluR6-S1S2 protein with the T690A ligand binding mutation. *Bottom*, quantification of Western blots from GluR6-S1S2 medium release experiments illustrating a reduction in release into medium as a result of the T690A LBD mutation (65.7 ± 8.1%, $n = 5$, $p < 0.05$). *wt*, wild type.

Interactions between Glutamate Binding and Disulfide Mutants—Elimination of glutamate binding and introduction of the disulfide bond in the LBD had opposing effects on secretion of the soluble GluR6a-S1S2 protein, but both mutations reduced PM localization of full-length kainate receptors. We next determined which alteration dominated the expression phenotype in LBDs with both mutations, which could reveal if glutamate binding was required for formation of an interdomain disulfide bond. As expected, relative PM expression of a full-length receptor with all three mutations, GluR6a(E441C/T690A/N721C), was reduced significantly relative to wild-type GluR6a receptors (13.9 ± 2.8%, $n = 8$, $p < 0.001$ *versus* 76.6 ± 9.0%, $n = 7$) to a level comparable with the GluR6a(T690A) mutant receptor (Fig. 3*A*, *bottom*). In contrast, secretion of the soluble triple mutant, GluR6-S1S2(E441C/T690A/N721C), was similar to that of wild-type GluR6-S1S2 (normalized secretion 105.5 ± 12% of wild-type, $n = 4$, not significant). This intermediate level was significantly more than the ligand binding mutant (GluR6-S1S2(T690A)) and less than the disulfide mutant (GluR6-S1S2(E441C/N721C)) protein secretion. These

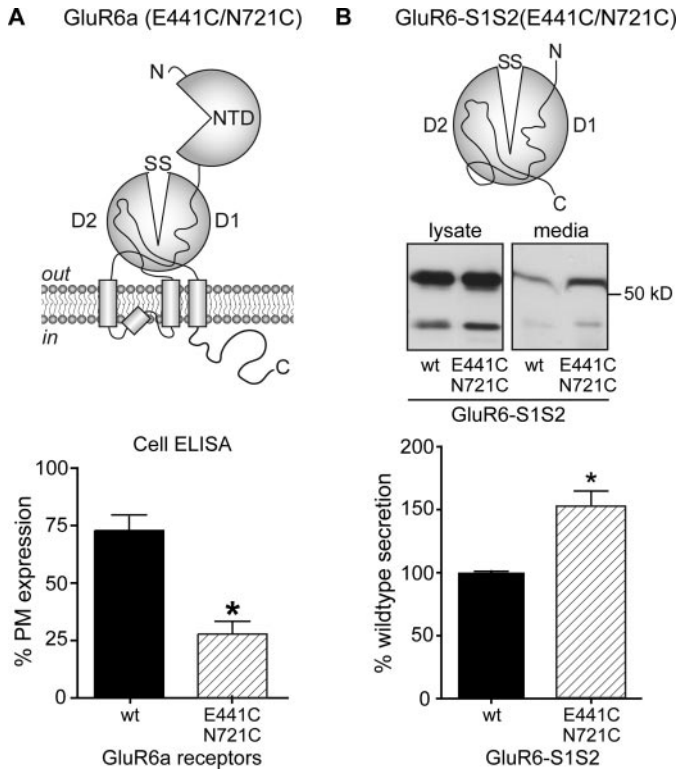

FIGURE 2. **An interdomain disulfide bond across the LBD reduces PM expression of GluR6a receptors.** *A*, *top*, diagram illustrating the full-length GluR6a receptor with the engineered disulfide bond. *Bottom*, quantification of cell ELISA data illustrating a reduction in PM expression resulting from the E441C/N721C mutation (27.8 ± 3.7%, $n = 14$ *versus* 75.4 ± 3.9%, $n = 13$, $p < 0.001$). *B*, *top*, diagram illustrating the soluble GluR6-S1S2 protein with the locked LBD mutation. *Bottom*, quantification of Western blots from GluR6-S1S2 medium release experiments illustrating an increase in release into medium as a result of the E441C/N721C LBD mutation (151.6 ± 11.9%, $n = 3$, $p < 0.05$). *wt*, wild type.

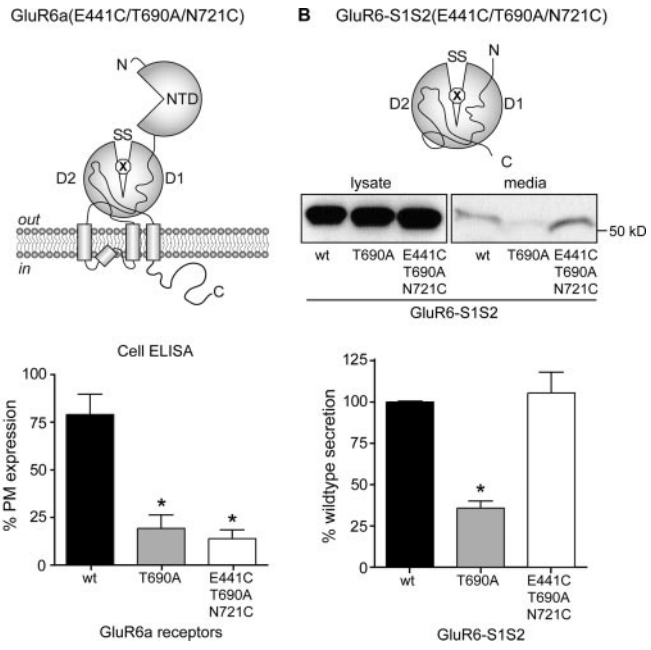

FIGURE 3. **Elimination of agonist binding prevents full expression of the disulfide mutant phenotype in the soluble LBD.** *A*, *top*, diagram illustrating the full-length GluR6a receptor with both the T690A ligand binding mutation and the engineered disulfide bond. *Bottom*, quantification of cell ELISA data illustrating a reduction in PM expression resulting from the ligand binding and the combined disulfide bond-forming and ligand binding mutations (T690A: 19.3 ± 6.0%, $n = 7$; E441C/T690A/N721C: 13.9 ± 2.8%, $n = 8$ *versus* 76.6 ± 9.0%, $n = 7$). *B*, *top*, diagram illustrating the soluble GluR6-S1S2 protein with both the T690A ligand binding mutation and the disulfide bond-forming LBD mutations. *Bottom*, quantification of Western blots from GluR6-S1S2 medium release experiments illustrating a decrease in release with the T690A ligand binding mutation but no change in release into medium as a result of the E441C/T690A/N721C mutations (T690A: 35.7 ± 3.4%, $n = 3$, $p < 0.001$; E441C/T690A/N721C: 105.5 ± 12%, $n = 4$). *wt*, wild type.

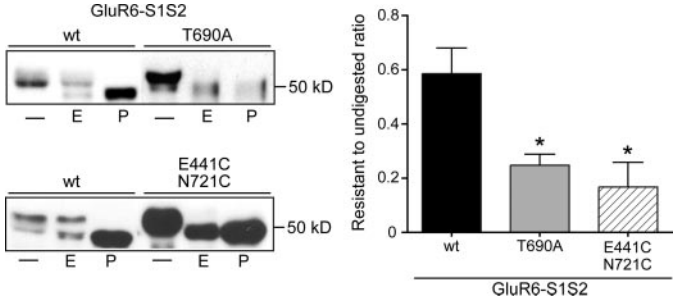

FIGURE 4. **The ligand binding and the disulfide LBD mutations prevent mature glycosylation of the soluble LBD.** Representative Western blot (*left*) and quantification (*right*) of Western blots from glycosidase resistance assays illustrating a reduced mature glycosylation of GluR6-S1S2(T690A) (0.25 ± 0.04, $n = 3$, $p < 0.05$) and GluR6-S1S2(E441C/N721C) (0.17 ± 0.1, $n = 3$, $p < 0.05$) relative to GluR6-S1S2 (0.59 ± 0.1, $n = 3$). −, conditions; *E*, endoglycosidase H; *P*, peptide:*N*-glycosidase F; *wt*, wild type.

data demonstrate that introduction of the disulfide bond alleviates the secretory deficit resulting from elimination of the glutamate binding site in the soluble S1S2 protein.

Glycosylation of LBD Proteins—We also examined the glycosylation state of the soluble S1S2 proteins to determine if their altered secretion was correlated with changes in oligosaccharide processing. Acquisition of resistance to the endoglycosidase H glycosidase, which cleaves immature oligosaccharide moieties, is a commonly used diagnostic assay to measure trafficking through the medial Golgi (10, 23–25). Secreted S1S2 proteins were analyzed on Western blots following digestion in either control conditions (−), endoglycosidase H glycosidase (*E*), or peptide:*N*-glycosidase F (a glycosidase that cleaves both immature and mature oligosaccharide moieties) (*P*) (Fig. 4). Wild-type GluR6-S1S2 protein exhibited >50% resistance to endoglycosidase H digest, whereas oligosaccharides on both GluR6-S1S2(T690A) and GluR6-S1S2(E441C/N721C) LBDs were digested by endoglycosidase H to near completion (25 ± 0.4 and 17 ± 0.9% resistance remaining, $n = 3$ assays each, $p < 0.05$) (Fig. 4). Thus, oligosaccharide processing appeared uncorrelated with secretion of the soluble proteins.

Functional Evidence for the Formation of an Interdomain Disulfide Bond—We confirmed the presence of an interdomain disulfide bond in whole cell patch clamp recordings from HEK293 T/17 cells transfected with either GluR6a or GluR6a(E441C/N721C) receptors. As shown in the representative *traces* in Fig. 5*A*, 100-ms applications of 10 mM glutamate elicited large amplitude, rapidly desensitizing currents from wild-type GluR6a KARs (mean 13.5 ± 2.0 nA, $n = 4$). Currents gated by GluR6a(E441C/N721C), in contrast, were <2% of the wild-type amplitude (231 ± 112 pA, $n = 5$), consistent with combined functional and localization deficits. The marked attenuation of glutamate-evoked currents, which was much greater than predicted by the cell ELISAs (Fig. 2*A*), could have resulted from inaccessibility of the binding site in the presence

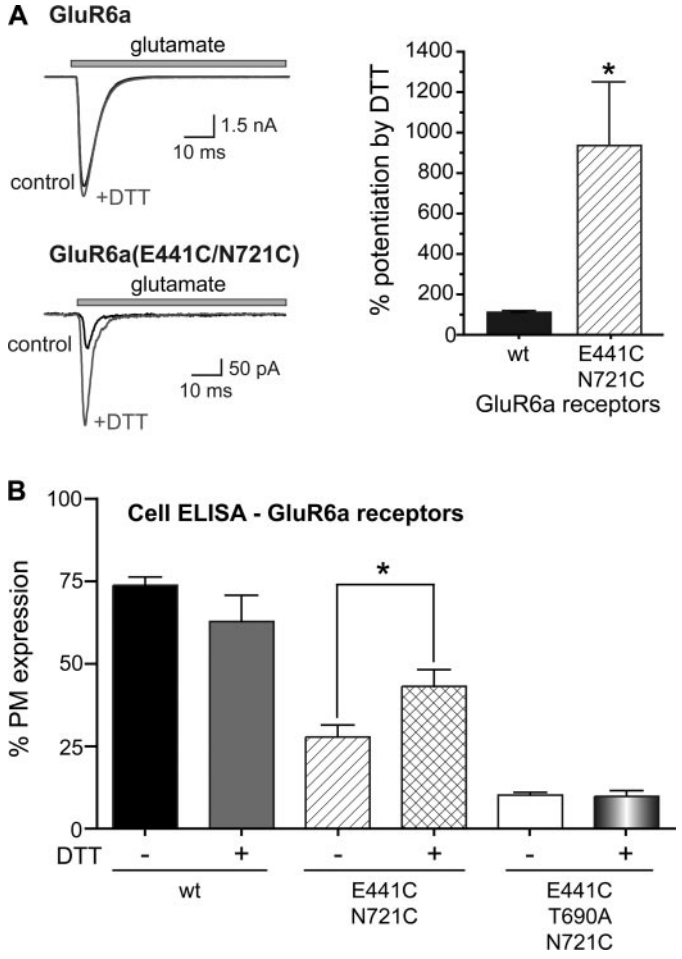

FIGURE 5. **DTT application provides functional evidence for the formation of an interdomain disulfide bridge**. *A*, representative traces (*left*) and quantitation (*right*) of whole cell peak currents elicited by a 100-ms application of 10 mM glutamate from wild-type GluR6a and GluR6a(E441C/N721C) reveal a significant potentiation of peak currents elicited with co-application of 5 mM DTT from GluR6a(E441C/N721C) when compared with wild-type GluR6a (928 ± 320%, $n = 4$ *versus* 110 ± 2%, $n = 5$, $p < 0.05$). *B*, quantification of cell ELISA data illustrating a selective and significant increase in PM expression of GluR6a(E441C/N721C) resultant from culturing in the presence of 1 mM DTT (E441C/N721C: 27.8 ± 3.7%, $n = 14$ *versus* 43.2 ± 5.0%, $n = 9$, $p < 0.05$; E441C/T690A/N721C: 10.2 ± 0.8%, $n = 7$ *versus* 9.8 ± 1.7%, $n = 7$; GluR6a: 73.8 ± 2.6%, $n = 13$ *versus* 62.8 ± 8.0%, $n = 3$). *wt*, wild type.

of an interdomain disulfide bond. Therefore, we co-applied 5 mM DTT with both external and glutamate solutions to reduce the disulfide bond; this treatment resulted in rapid potentiation of glutamate-evoked peak currents gated by the GluR6a(E441C/N721C) but not wild-type GluR6a receptors (potentiation from pre-DTT amplitudes of 928 ± 320% *versus* 110 ± 2%, respectively, $n = 4$ and 5 recordings, $p < 0.05$), confirming that the disulfide bond was present in the nonreduced receptor and occluded access of glutamate to the binding cleft. Interestingly, currents decreased rapidly to initial preapplication amplitudes following the removal of DTT, suggesting that the interdomain disulfide bond readily oxidized to restrict the LBDs.

We next tested if the reduced trafficking and membrane localization of GluR6a(E441C/N721C) receptors were reversible upon reduction of the disulfide bond. Receptor-expressing cells were cultured for 16 h in 1 mM DTT before cell ELISAs were performed to quantitate relative PM localization. DTT incubation had no effect on GluR6a relative PM expression (without DTT, 73.8 ± 2.6%, $n = 12$; with DTT, 62.8 ± 8.0%, $n = 3$) (Fig. 5*B*). Surface expression of GluR6a(E441C/N721C) receptor, however, was significantly increased by DTT, from 27.8 ± 3.7% to 43.2 ± 5.0%, $n = 14$ and 9, respectively, $p < 0.05$). The triple mutant, GluR6a(E441C/T690A/N721C), did not exhibit the same increase with DTT (control, 10.2 ± 0.8%; DTT, 9.8 ± 1.7%; $n = 7$ for each condition) (Fig. 5*B*). Thus, membrane expression is enhanced by reduction of the interdomain disulfide bond, consistent with a biogenic requirement for flexibility of the LBD.

Impact of the Interdomain Disulfide Bridge on Oligomerization—Mutagenic restriction of the LBD dynamics in the GluR6a(E441C/N721C) receptor could reduce PM expression through a number of mechanisms, including inefficient subunit folding, altered multimeric assembly, or a specific impact on receptor trafficking. Western blot analysis of membrane lysates revealed that GluR6a(E441C/N721C) subunit protein was expressed at dramatically lower levels than wild-type GluR6a subunits (Fig. 6*A*). This was similarly observed in native PAGE analysis of oligomerization (Fig. 6*B*). At 18 and 24 h post-transfection of COS-7 cells, wild-type GluR6a receptors were found in monomeric and tetrameric states, as was observed in a previous study (7). In contrast, the small amount of GluR6a(E441C/N721C) receptor detectable at 18 h post-transfection is present as monomers and dimers. A similar stoichiometric distribution is observed at 24 h post-transfection; tetrameric bands were largely absent. Quantitation of oligomeric bands via densitometry revealed that GluR6a(E441C/N721C) receptors exhibited a ~5-fold increase in the ratio of dimers to tetramers relative to GluR6a receptors (GluR6, 0.89 ± 0.1; GluR6a(E441C/N721C), 4.9 ± 2.7, $n = 3$ assays, $p < 0.05$) (Fig. 6*B*). No significant difference was observed in the ratio of monomers to dimers. Therefore, the disulfide bridge impacts association of dimers during receptor assembly.

Analysis of Receptor Folding—Last, we assessed the impact of loss of glutamate binding or introduction of the interdomain disulfide bridge on protein folding. In the first set of experiments, we measured the ER mobility of GFP-tagged GluR6a, GluR6a(T690A), and GluR6a(E441C/N721C) receptors using fluorescence recovery after photobleaching analysis, because misfolded proteins (including glutamate receptors) exhibit slower rates of diffusion in conditions of ATP depletion (19, 20). We depleted transfected COS-7 cells of ATP via incubation with 2-deoxyglucose and then measured the time course of fluorescence recovery within photobleached areas of transfected cells (Fig. 7*A*). GFP-GluR6a and GluR6a(E441C/N721C) receptors had similar recovery kinetics (GluR6a $t_{1/2}$ = 20.4 ± 1.9 s; GluR6a(E441C/N721C) $t_{1/2}$ = 21.6 ± 1.7 s; $n = 12$ and 13 cells analyzed, respectively) (Fig. 7, *B* and *C*), but GluR6a(T690A) recovered fluorescence significantly more slowly (30.5 ± 1.9 s, $n = 13$, $p < 0.01$) (Fig. 7, *B* and *C*). This slower recovery was reflected in a smaller estimated diffusion coefficient for GluR6a(T690A) (0.082 ± 0.006 $\mu m^2/s$, $n = 13$, $p < 0.05$) compared with GluR6a and GluR6a(E441C/N721C) (0.110 ± 0.010 and 0.113 ± 0.008 $\mu m^2/s$, respectively) (Fig. 7*D*). To ensure that this reduction in ER mobility was not the result of a reduced

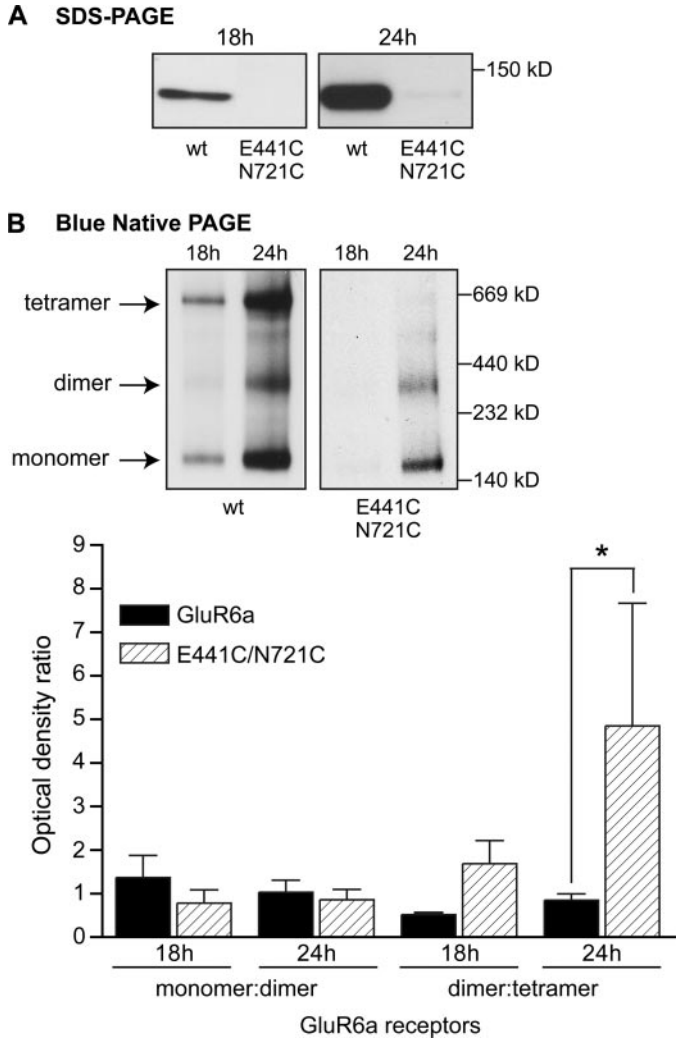

FIGURE 6. **Locking the LBD disrupts GluR6a oligomeric assembly.** *A*, representative Western blots illustrate reduced expression of the locked LBD GluR6a mutant compared with wild-type GluR6a at 18 and 24 h post-transfection. *B*, *top*, representative BN-PAGE Western blots at 18 and 24 h of GluR6a (*left*) and GluR6a(E441C/N721C) (*right*) receptors. *Bottom*, quantification of BN-PAGE Western blots illustrates disruption in the oligomeric assembly for GluR6a(E441C/N721C) with a significant increase in the dimer/tetramer ratio compared with the GluR6a (4.9 ± 2.7, $n = 3$ *versus* 0.89 ± 0.1, $n = 3$, $p < 0.05$). *wt*, wild type.

mobile receptor pool, we compared the mobile fractions for GluR6a, the ligand-binding mutant, and the disulfide-locked mutant and found no difference among the three receptors (58.1 ± 2.6, 55.6 ± 2.8, and 56.1 ± 2.7%, $n = 13$, 17, and 14, respectively) (Fig. 7*E*).

As a second comparison of protein folding, we measured association of GluR6a(E441C/N721C) subunits with the folding-associated ER chaperone calnexin. Previously, GluR6a(T690A) receptors had increased association with this protein relative to wild-type GluR6a receptors, suggestive of receptor misfolding (7, 14). Immunoprecipitations from transfected COS-7 cells were carried out with anti-calnexin antibody before immunoblotting for anti-Myc immunoreactivity. In contrast to GluR6a(T690A), GluR6a(E441C/N721C) (81 ± 30%, $n = 3$) receptors were not associated with calnexin to any greater degree than wild-type GluR6a receptors.

Calnexin association with S1S2 soluble proteins also was assayed to determine if alterations in secretion could be attributed to misfolding. Western blots and densitometric analysis of immunoprecipitated proteins revealed a significant increase in the amount of GluR6-S1S2(T690A) (by 255 ± 33%, $n = 3$, $p < 0.01$) associated with calnexin relative to wild-type GluR6-S1S2 (Fig. 8, *A* and *B*). No significant change from wild type was observed with GluR6-S1S2(E441C/N721C) (144 ± 19%).

Taken together, these results support the hypothesis that decreased PM expression of the T690A mutant receptor in part results from misfolding of the LBD, whereas the decreased expression of the disulfide LBD mutant receptor is a consequence of defective assembly with no apparent folding deficits.

DISCUSSION

Biogenesis and assembly of glutamate receptors are critical early determinants of ionotropic glutamate receptor function and subcellular localization. We show here that glutamate binding within the ER is essential for the proper folding of the GluR6a KAR ligand-binding domain. Furthermore, these results demonstrate that relaxation from the closed, glutamate-bound conformation is necessary for assembly and trafficking of GluR6a, consistent with the hypothesis that GluR6a KARs undergo critical conformational transitions early in receptor assembly. These data support the hypothesis that key ER quality control checkpoints occur during subunit folding and oligomerization, prior to full assembly of export-competent KARs. The dimer-to-tetramer transition could represent a common early biogenic checkpoint, because assembly of AMPA and kainate receptors possessing defects in ligand binding (7, 10), gating transitions (7, 9), and conformationally restricted LBDs are impacted at this stage in biogenesis. The results of this study suggest that glutamate may act as a molecular chaperone necessary for the proper folding of the ligand-binding domain and that ER quality control processes are engaged critically at an early stage of receptor biogenesis rather than on fully assembled tetrameric receptors.

Glutamate Binding, Pre- or Postassembly Checkpoint?—The importance of intracellular glutamate binding for PM expression was first shown for glutamate receptor analogues in *Caenorhabditis elegans* (13). For mammalian AMPA and KA receptors, elimination of glutamate binding reduces forward trafficking to the PM in heterologous cells and transfected neurons (10, 14–16). In addition to glutamate binding, receptors that are blocked from entering a desensitized state (8), have altered desensitization kinetics (26), or are mutated at key dimerization residues (14, 26) have reduced cell surface expression. The inverse correlation of these physiological deficits and PM expression gave rise to the hypothesis that functionality of the nascent receptors was sampled by intracellular quality control systems in the ER (2, 8, 14, 27).

Based on our current results, we propose instead that reductions in PM localization can be accounted for in large part by subunit misfolding or inefficient oligomerization of receptors rather than an intracellular test on functional, export-competent receptors. Changes to the LBD alone were sufficient to reduce PM expression, since both the full-length GluR6a(T690A) and the soluble GluR6-S1S2(T690A) protein

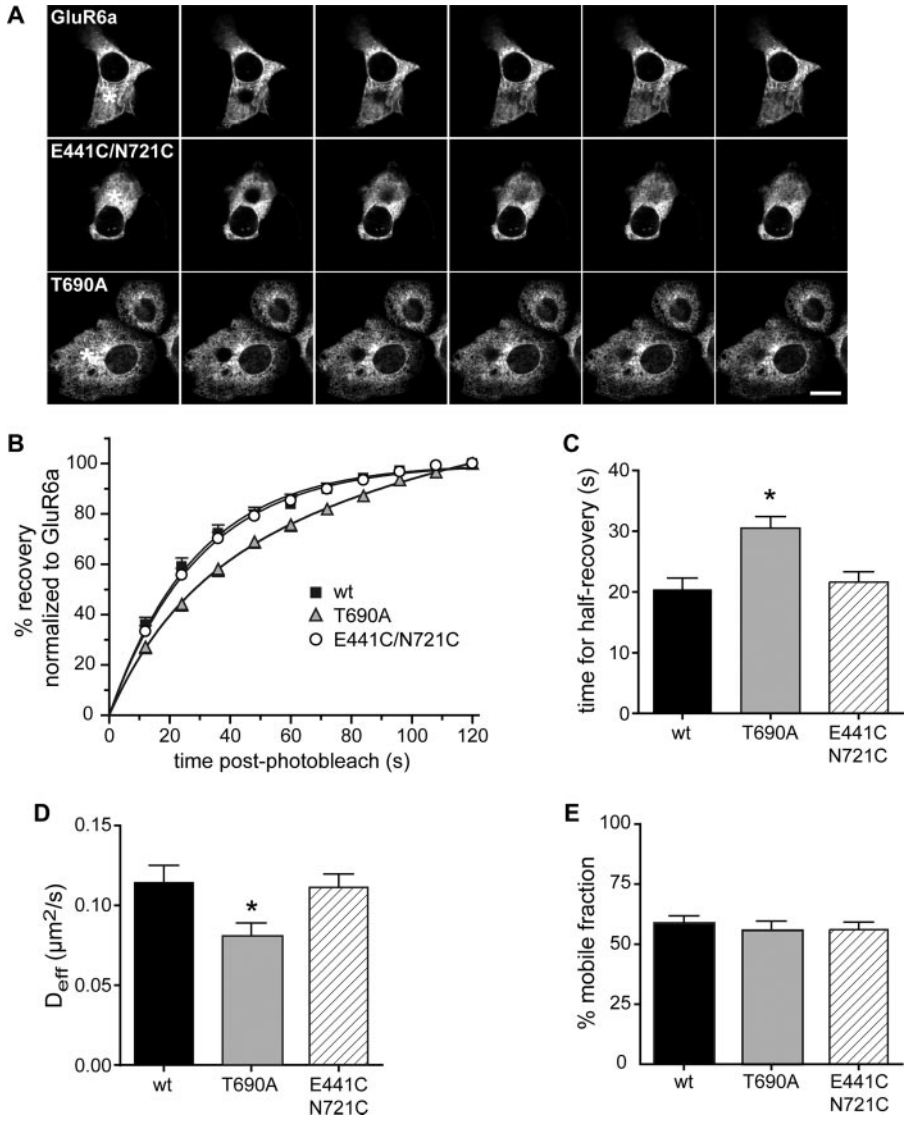

FIGURE 7. **The elimination of glutamate binding reduces ER receptor mobility.** *A*, representative confocal micrographs, taken immediately prior to, immediately after, and every 12 s after photobleaching of GluR6a (*top*), GluR6a(E441C/N721C) (*middle*), and GluR6a(T690A) (*bottom*), demonstrating mobility of the GFP-tagged protein after photobleaching. *Scale bars*, 20 μm. *B*, graph of the fractional fluorescence recovery for wild-type and mutant GFP-tagged receptors. *C*, analysis of the time for half-recovery of fluorescence within the photobleached area shows that $t_{1/2}$ for GluR6a(T690A) but not GluR6a(E441C/N721C) was increased compared with wild-type GluR6a (T690A: 30.5 ± 1.9 s, $n = 13$, $p < 0.01$; E441C/N721C: 21.6 ± 1.7 s, $n = 13$ *versus* 20.4 ± 1.9 s, $n = 12$). *D*, analysis of the effective diffusion coefficients reveals a significant decrease in the mobility of GluR6a(T690A) but not GluR6a(E441C/N721C) compared with GluR6a (T690A: 0.082 ± 0.006 $\mu m^2/s$, $n = 13$, $p < 0.05$; E441C/N721C: 0.113 ± 0.008 $\mu m^2/s$, $n = 12$ *versus* 0.11 ± 0.01 $\mu m^2/s$, $n = 12$). *E*, quantitation of the mobile fraction revealed no significant difference between GluR6a (58.1 ± 2.6%, $n = 13$), GluR6a(E441C/N721C) (56.1 ± 2.7%, $n = 14$) and GluR6a(T690A) (55.6 ± 2.8%, $n = 17$). *wt*, wild type.

had reduced PM expression and secretion, respectively (Fig. 1). Also, the T690A LBD mutation reduced ATP-dependent ER mobility (Fig. 7) and increased association with the ER chaperone, calnexin (Fig. 8), which suggests that glutamate, acting in a chaperone-like manner, is necessary for proper folding of the LBD. A similar form of ligand-dependent stabilization of folding intermediates of nascent proteins was postulated to occur during biogenesis of the vasopressin V_2 receptor, the δ-opioid receptor, and the NR1–1a NMDA receptor subunit (11, 28, 29). The difference in the severity of the deficit between PM expression of the full-length receptor and secretion of the soluble LBD with the ligand binding mutation could reflect additional conformational changes promoted by glutamate binding, such as exposure of residues involved in dimerization within the full-length receptor. GluR2 AMPAR ligand binding mutants exhibit increased misfolding and reduced forward trafficking (9), and a similar "chaperone-like" activity for glutamate binding was proposed recently for GluR4 AMPA receptors based on thermodynamic data that demonstrated increased structural stability of the LBD in the presence of glutamate (15, 30).

In addition to compromising subunit folding, elimination of glutamate binding disrupts homo-oligomeric assembly of GluR6a KARs receptors (7) and might have an equivalent effect in AMPA receptors (2, 9, 27). Mutations that alter receptor kinetics in AMPA and KARs (7, 9) as well as GluR2 receptors with reduced LBD interface stability (9) also negatively affect forward trafficking through increasing misfolding and, at least for GluR6a, disrupt receptor oligomerization at the dimer-to-tetramer transition (7). Together, these data support the hypothesis that ER quality control engages AMPA and KAR early in receptor biogenesis with much of the observed reductions in PM expression attributed to defects at pretetrameric stages rather than on fully assembled, functional receptors.

Multiple GluR6a Conformational Changes Precede Tetrameric Assembly—Glutamate binding appears to be required for membrane expression for glutamate receptors (10, 14–16), but the mechanistic basis for this phenomenon has been unclear. One possibility is that binding induces a specific conformational state, a closed LBD, permissive for ER exit. We tested this hypothesis by stabilizing the conformational state through introduction of an interdomain disulfide bond and measuring the effect on receptor trafficking. The results of this study suggested that an inflexible closed state is not the only conformational transition made in GluR6a receptor biogenesis and transit to the PM. Formation of the interdomain disulfide bond reduced PM expression (Fig. 2), and reduction of the disulfide bond partially reversed the trafficking phenotype (Fig. 5). In contrast to the glutamate binding mutant, the presence of the disulfide bond did not induce misfolding of the mutant receptor (Figs. 7 and 8) but did disrupt

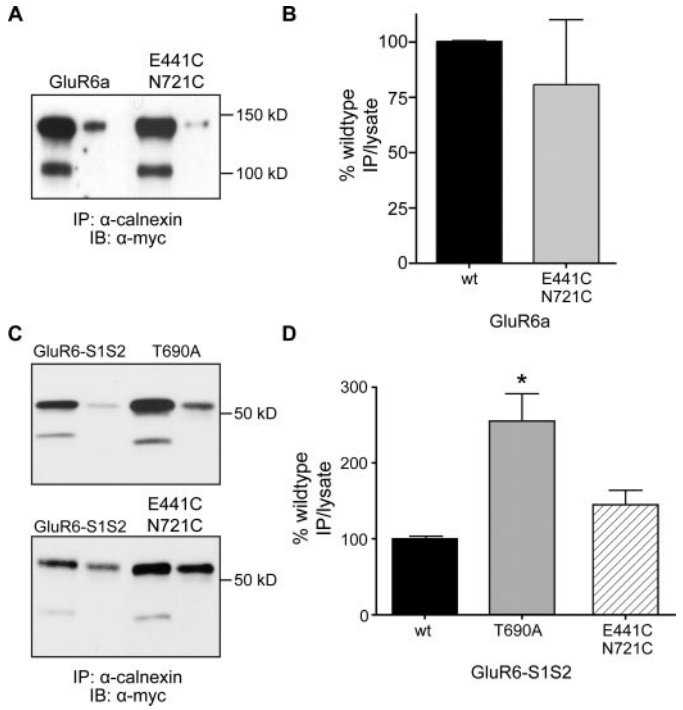

FIGURE 8. **The ligand binding mutation but not the disulfide bond across the LBD increases association with the ER chaperone, calnexin.** *A*, representative Western blots (*IB*) of lysate and calnexin-immunoprecipitated (*IP*) proteins from GluR6a- and GluR6a(E441C/N721C)-transfected COS-7 cells. *B*, quantification of Western blots reveals no increased association of GluR6a(E441C/N721C) with calnexin relative to GluR6a (E441C/N721C: 81 ± 30%, $n = 3$). *C*, representative Western blots of lysate and calnexin-immunoprecipitated proteins from GluR6-S1S2(T690A)-transfected (*top*) and GluR6-S1S2(E441C/N721C)-transfected (*bottom*) COS-7 cells compared with lysate and calnexin-immunoprecipitated proteins from wild-type transfected cells. *D*, quantification of Western blots reveals an increased association of GluR6-S1S2(T690A) but not GluR6-S1S2(E441C/N721C) with calnexin relative to GluR6-S1S2 (T690A: 255 ± 33%, $n = 3$, $p < 0.01$; E441C/N721C: 144 ± 19%, $n = 3$). *wt*, wild type.

oligomeric assembly (Fig. 6). Furthermore, we infer that conformational changes associated with relaxation from the glutamate-bound state involved domains other than the LBD, because secretion of soluble LBDs possessing the disulfide bond was increased relative to the wild-type soluble LBD (Fig. 2) despite possessing an immature glycosylation phenotype (Fig. 4). This decrease in endoglycosidase H resistance could be a consequence of inaccessibility of the glycosylation sites in the restricted conformation. Consistent with these findings, an analogous interdomain disulfide bond in the GluR2 AMPA receptor subunit, which restricted conformational changes, also reduced forward trafficking, but the folding and assembly properties of this mutant were not examined (9).

Functional Impact of Disulfide Restriction of the GluR6 LBD—The functional consequences of introducing the interdomain disulfide bridge in GluR6a receptors contrasted with those observed upon analogous mutation of NMDA receptors; *i.e.* dual cysteine mutation to create interdomain disulfide bridges in NR1/NR2 heteromeric receptors produced constitutively active channels (31). Disulfide-bonded mutant GluR6a receptors, however, gated very little current, much less than anticipated from the 30% surface expression measured in ELISAs. Reduction of the disulfide bond reversibly potentiated the glutamate-evoked currents by ~10-fold (Fig. 5). Reformation of the disulfide bridge appeared to be use-independent, because current amplitudes were diminished rapidly upon wash-out of DTT (data not shown), consistent with the idea that transient LBD closures occur in the absence of stabilizing ligand interactions. This physiological behavior could arise from several possible underlying mechanisms. First, the binding site might be occluded initially in the oxidized disulfide mutants, only becoming accessible as the reducing agent "unlocked" the receptors. We note, however, that agonist application onto constitutively active NMDA receptors with analogous mutations increased currents, suggesting that the disulfide bond in that instance did not completely prevent agonist binding or dissociation (31). Alternatively, the presence of the interdomain disulfide bond in GluR6 might induce a highly desensitized state of the receptor (either with or without agonist bound), which would account for the small initial amplitude of currents. Application of DTT and reduction of the interdomain disulfide bonds would permit recovery from desensitization, leading to the observed "potentiation" (Fig. 5). Differences in the magnitude of basal desensitization induced by the disulfide bridge mutation in NMDA *versus* GluR6 KARs may account for the distinct physiological activities.

In conclusion, we determined that agonist binding is essential not only for the PM expression of GluR6a but also for the folding of the LBD itself. In addition, we show here that the LBD of GluR6a at least must undergo conformational relaxation for efficient assembly and trafficking of nascent GluR6a receptors to the PM, consistent with the model proposed for AMPA receptors (9). Critical ER quality control checkpoints occur early in receptor oligomeric assembly, at the dimer-to-tetramer transition, which is negatively impacted by several functionally relevant mutations (*i.e.* elimination of glutamate binding, altered desensitization, and relaxation from a glutamate-bound state). Thus, appropriate biogenesis is assessed at multiple early stages by cellular systems that prevent aberrant iGluR expression and function.

Acknowledgments—We thank the Northwestern University Feinberg School of Medicine Cell Imaging Facility for training in fluorescence recovery after photobleaching analysis.

REFERENCES

1. Pinheiro, P., and Mulle, C. (2006) *Cell Tissue Res.* **326,** 457–482
2. Greger, I. H., and Esteban, J. A. (2007) *Curr. Opin. Neurobiol.* **17,** 289–297
3. Hirbec, H., Francis, J. C., Lauri, S. E., Braithwaite, S. P., Coussen, F., Mulle, C., Dev, K. K., Coutinho, V., Meyer, G., Isaac, J. T., Collingridge, G. L., and Henley, J. M. (2003) *Neuron* **37,** 625–638
4. Luscher, C., Xia, H., Beattie, E. C., Carroll, R. C., von Zastrow, M., Malenka, R. C., and Nicoll, R. A. (1999) *Neuron* **24,** 649–658
5. Luthi, A., Chittajallu, R., Duprat, F., Palmer, M. J., Benke, T. A., Kidd, F. L., Henley, J. M., Isaac, J. T., and Collingridge, G. L. (1999) *Neuron* **24,** 389–399
6. Park, Y., Jo, J., Isaac, J. T., and Cho, K. (2006) *Neuron* **49,** 95–106
7. Vivithanaporn, P., Lash, L. L., Marszalec, W., and Swanson, G. T. (2007) *J. Neurosci.* **27,** 10423–10433
8. Priel, A., Selak, S., Lerma, J., and Stern-Bach, Y. (2006) *Neuron* **52,** 1037–1046
9. Penn, A. C., Williams, S. R., and Greger, I. H. (2008) *EMBO J.* **27,** 3056–3068
10. Mah, S. J., Cornell, E., Mitchell, N. A., and Fleck, M. W. (2005) *J. Neurosci.*

25, 2215–2225
11. Kenny, A. V., Cousins, S. L., Pinho, L., and Stephenson, F. A. (2009) *J. Biol. Chem.* **284,** 324–333
12. Valluru, L., Xu, J., Zhu, Y., Yan, S., Contractor, A., and Swanson, G. T. (2005) *J. Biol. Chem.* **280,** 6085–6093
13. Grunwald, M. E., and Kaplan, J. M. (2003) *Neuropharmacology* **45,** 768–776
14. Fleck, M. W. (2006) *Neuroscientist* **12,** 232–244
15. Coleman, S. K., Moykkynen, T., Jouppila, A., Koskelainen, S., Rivera, C., Korpi, E. R., and Keinanen, K. (2009) *J. Neurosci.* **29,** 303–312
16. Greger, I. H., Akamine, P., Khatri, L., and Ziff, E. B. (2006) *Neuron* **51,** 85–97
17. Schiffer, H. H., Swanson, G. T., and Heinemann, S. F. (1997) *Neuron* **19,** 1141–1146
18. Wittig, I., Braun, H. P., and Schagger, H. (2006) *Nat. Protoc.* **1,** 418–428
19. Atlason, P. T., Garside, M. L., Meddows, E., Whiting, P., and McIlhinney, R. A. (2007) *J. Biol. Chem.* **282,** 25299–25307
20. Snapp, E. L., Altan, N., and Lippincott-Schwartz, J. (2003) *Current Protocols in Cell Biology*, pp. 21.1.1–21.1.24, John Wiley and Sons, Hoboken, New Jersey
21. Axelrod, D., Koppel, D. E., Schlessinger, J., Elson, E., and Webb, W. W. (1976) *Biophys. J.* **16,** 1055–1069
22. Mayer, M. L. (2005) *Neuron* **45,** 539–552
23. Vazhappilly, R., and Sucher, N. J. (2002) *Neurosci. Lett.* **318,** 153–157
24. Selkirk, J. V., Challiss, R. A., Rhodes, A., and McIlhinney, R. A. (2002) *J. Neurochem.* **80,** 346–353
25. Matsuda, S., Hannen, R., Matsuda, K., Yamada, N., Tubbs, T., and Yuzaki, M. (2004) *Eur. J. Neurosci.* **19,** 1683–1690
26. Fleck, M. W., Cornell, E., and Mah, S. J. (2003) *J. Neurosci.* **23,** 1219–1227
27. Greger, I. H., Ziff, E. B., and Penn, A. C. (2007) *Trends Neurosci.* **30,** 407–416
28. Morello, J. P., Petaja-Repo, U. E., Bichet, D. G., and Bouvier, M. (2000) *Trends Pharmacol. Sci.* **21,** 466–469
29. Petaja-Repo, U. E., Hogue, M., Bhalla, S., Laperriere, A., Morello, J. P., and Bouvier, M. (2002) *EMBO J.* **21,** 1628–1637
30. Madden, D. R., Abele, R., Andersson, A., and Keinanen, K. (2000) *Eur. J. Biochem.* **267,** 4281–4289
31. Blanke, M. L., and VanDongen, A. M. (2008) *J. Biol. Chem.* **283,** 21519–21529